

AD-A119 853

FOREIGN TECHNOLOGY DIV WRIGHT-PATTERSON AFB OH  
A RADIAL ELECTRON BEAM FOR PUMPING LASERS. (U)  
SEP 82 G QI, X SHANSHAN, W YUEPO, W PEIGANG  
FTD-ID(RS)T-0789-82

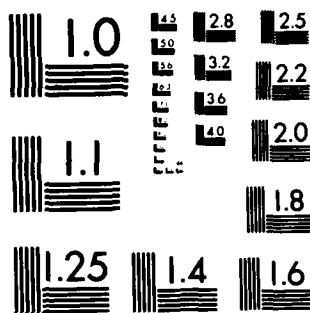
UNCLASSIFIED

F/6 20/7

1/1

NL

END  
041  
FILMED  
2 83  
DTIC



MICROCOPY RESOLUTION TEST CHART  
NATIONAL BUREAU OF STANDARDS-1963-A

AD-A119 853

FTD-ID(RS)T-0980-82

FTD-ID(RS)T-0789-82

## FOREIGN TECHNOLOGY DIVISION



A RADIAL ELECTRON BEAM FOR PUMPING LASERS

by

Ge Qi, Xu Shanshan, et al

DTIC FILE COPY



DTIC  
ELECTE  
S JAN 31 1983 D  
D

Approved for public release;  
distribution unlimited.



83 01 31 146

FTD-ID(RS)T-0980-82

## EDITED TRANSLATION

FTD-ID(RS)T-0980-82

9 December 1982

MICROFICHE NR: FTD-82-C-001652

A RADIAL ELECTRON BEAM FOR PUMPING LASERS

By: Ge Qi, Xu Shanshan, et al

English pages: 12

Source: Dianzi Xuebao Vol. 3, Nr. 1,  
January 1981, pp. 39-44

Country of origin: China  
Translated by: LEO KANNER ASSOCIATES  
F33657-81-D-0264

Requester: FTD/TQTD

Approved for public release; distribution unlimited.



Accession Per	
NTIS GRA&I	<input checked="" type="checkbox"/>
DTIC TAB	<input type="checkbox"/>
Unannounced	<input type="checkbox"/>
Justification	
By	
Distribution/	
Availability Codes	
Dist	Avail and/or Special
A	

THIS TRANSLATION IS A RENDITION OF THE ORIGINAL FOREIGN TEXT WITHOUT ANY ANALYTICAL OR EDITORIAL COMMENT. STATEMENTS OR THEORIES ADVOCATED OR IMPLIED ARE THOSE OF THE SOURCE AND DO NOT NECESSARILY REFLECT THE POSITION OR OPINION OF THE FOREIGN TECHNOLOGY DIVISION.

PREPARED BY:

TRANSLATION DIVISION  
FOREIGN TECHNOLOGY DIVISION  
WP.AFB, OHIO.

FTD-ID(RS)T-0980-82

Date 9 Dec 19 82

**GRAPHICS DISCLAIMER**

**All figures, graphics, tables, equations, etc. merged  
into this translation were extracted from the best  
quality copy available.**

## A RADIAL ELECTRON BEAM FOR PUMPING LASERS

by Ge Qi, Xu Shanshan, Wang Yuepo and Wang Peigang  
(Institute of Electronics, Academia Sinica)

### Abstract

This paper investigates the use of the radial relativistic electron beam for pumping a gas laser. It gives design and experimental results of a coaxial electron gun for the production of a radial electron beam. A preliminary discussion of certain characteristics of this type of beam are given. Further, this electron beam is used to successfully obtain laser output in the ultraviolet region.

### Preface

When the wavelength of a laser enters ultraviolet, vacuum ultraviolet and even shorter wavelengths, photon energy  $\hbar\nu$  becomes increasingly longer. When a solid or liquid is used as the laser medium, it also becomes more and more non-transparent. At this time, gas or steam is used more often as the laser medium. Aside from this, with the rise of conventional discharge, aerodynamic and chemical heat measures it is difficult to fulfill the requirements for pumping energy. Therefore, hollow cathode discharge with high energy electrons (energy greater than 10eV) and transverse fast discharge are often used. A high energy (energy greater than 0.3MeV) particle beam (e.g. electron, proton, ion and other particle beams) is also used as the pumping measure.

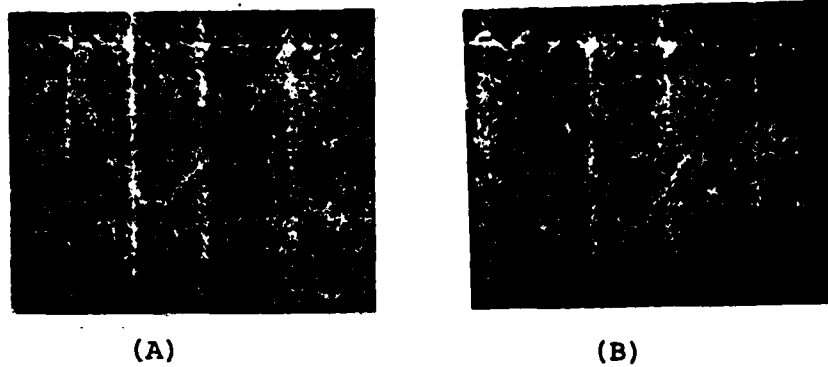
An electron beam is easily realized in a high energy

particle beam and a high beam flow density is also easily attained. Electrons are the same as other particles in that they do not sustain the laser medium's discharge characteristics, for example, the medium's  $E/p$  limitation and electric arc effects etc. When we compare electron pumping and discharge pumping, not only is the laser energy of a single pulse greater but the average power of the laser output when working at continuous pulse is also higher. The rapid development of electron beam technology has caused electron beam pumping to become a relatively ideal and reliable method for the present research of gas lasers.

Vertical, horizontal and radial electron beams are used for pumping lasers. Among these, the radial electron beam possesses an electron beam with high utilization ratio, good uniformity and large absorption of electron energy by the medium [1]. It can not only realize small volume, high gas pressure and short pulse strong pumping but can also realize large volume, quasi-large gas pressure and long pulse weak pumping [2]. As a result, it can attain large power and great energy laser output.

#### Experiment Device

We used a Marx generator with 600kV, 6kA, 40ns (FWHM) as the power source. It was remade from the power source of a 400kVX ray high speed camera. Starting from Paschen's Law and the room spectrum spark resistance theory [4], we increased the charging voltage of each level of the Marx generator as well as the gas pressure of the insulating gas to raise the output from 400kV to 600kV. At this time, the internal resistance of the Marx generator remains basically unchanged and when compared with the situation of increased progression, it is still located in a low resistance state (about 100  $\Omega$ ). As a result, the impedance of the electron gun (generally several ten ohm) easily matches it. The typical voltage and electric current waveform of the Marx generator are shown in fig. 1.



(A)

(B)

Fig. 1 Output Voltage and Electric Current Waveform of the Marx Generator. Time Scale is 10ns.

- (a) Voltage waveform
- (b) Electric current waveform

The experiment device is as shown in fig. 2.

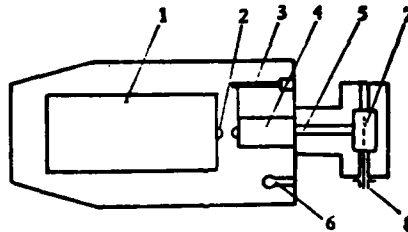


Fig. 2 Schematic of Experiment Device

Key:

- 1. Marx generator
- 2. Spark gap
- 3. Resistance voltage divider
- 4. Power source lead
- 5. Electron gun lead
- 6. Integrating ring
- 7. Electron gun
- 8. Faraday probe

The high pressure millimicrometer electric pulse of the Marx generator's output is added to the coaxial electron gun through leads 4 and 5 and produces a radial electron beam. When

designing leads 4 and 5, we should view them as internal conductors of the coaxial transmission line. Their characteristic impedance matches the internal resistance of the Marx generator. During manufacture, it is necessary to consider the breakdown characteristics of the high pressure millimicrometer electric pulse in insulated gas and in a vacuum [4]. The voltage and total current are separately measured by a resistance voltage divider and an integrating ring. The electron beam which goes through the cathode and enters the gas chamber is measured by the Faraday probe and acid-sensitive allochromatic sheets. The voltage and electric current waveforms are measured by a 100 MHz domestic made high voltage oscilloscope.

#### Production of the Radial Electron Beam

The radial electron beam is produced by a coaxial electron gun. This type of electron gun is composed of a coaxial cylindrical cathode and anode as shown in fig. 3.

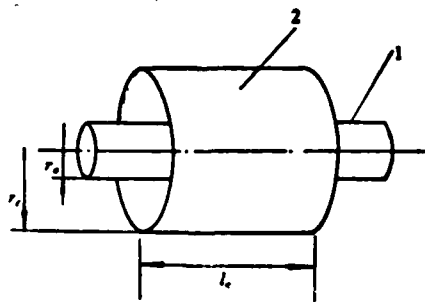


Fig. 3 Schematic of Coaxial Electron Gun

Key:  
 1. Anode  
 2. Cathode

Langmuir [5] gave the non-relativistic current formula of the cylinder diode space charge limit as:

$$I = 1.47 \times 10^4 \frac{V^{3/2}}{\eta^2 r_s} I_0 \quad (1)$$

In the formula

$$\eta = \epsilon - \frac{2}{5} \epsilon^2 + \frac{11}{120} \epsilon^3 - \frac{47}{3300} \epsilon^4 + 0.00168 \epsilon^5 + \dots,$$

$$\epsilon = \ln \frac{r_a}{r_c};$$

$l_c$  is the cathode's length (cm);  $r_a$  is the anode's radius (cm);  $r_c$  is the cathode's radius (cm);  $V$  is the voltage (MV);  $I$  is the current (A). From this, we obtain the electron gun's impedance:

$$Z_D = \frac{\eta^2 r_a}{l_c} V^{-1/2} \frac{10^3}{1.47} (\Omega) \quad (2)$$

At high voltage ( $>0.5$  MV), this type of cold cathode emission should take into account two types of corrections:

(1) At this time, after the speed of the electrons is accelerated between the anode and cathode of the electron gun, it can be compared to the speed of light. Therefore, we must consider the correction of the relativistic factors. Reference [6] gives the voltage correction for formula (1), that is, we substituted  $1.2 (\sqrt{V} - 0.85)^2$  for  $V^{3/2}$ . In this expression,  $\gamma$  is the relativistic factor.

(2) There are often many microburrs on the surface of this type of cold cathode. Thus, local field emission is produced under high field strength. Moreover, during the emission process, the resulting burr rapidly explodes, vaporizes and forms metallic plasma. The current of the electron gun is then emitted from the virtual cathode surface formed from this plasma. This plasma is dispersed towards the cathode at a speed of  $2-5$  cm/ $\mu$ s. In this way, it is necessary to have a correction item so that the cathode and anode distance changes with the time. Yet, this correction item can be overlooked for the short pulse (several to several tens of millimicroseconds) which we used.

Each of the parameters of the electron gun should be determined according to the power source impedance as well as the gain coefficient and excitation strength of the pumped laser. We can determine the length of the activation area, that is the length of the cathode  $l_c$ , from the laser's gain coefficient; we can determine the surface area of the anode from the current density required for pumping the laser and thus obtain anode radius  $r_a$ ; we can determine the electron gun's voltage  $V$  from the electron beam energy required to pump the laser. From a matching principle, that is starting from the fact that the electron gun's impedance  $Z_D$  should be the same as the internal impedance of the Marx generator, the radius of the cathode  $r_c$  can be obtained from expression (2). The calculation values and test results are listed in table 1. The two are quite similar.

$r_a$ (cm)	$r_c$ (cm)	$l_c$ (cm)	$V$ (kV)	$Z_D$ ( $\Omega$ )(1)	$Z_{MK}$ ( $\Omega$ )(2)
0.275	1.70	7.00	494	56.64	55.98

Table 1 Comparison of the Calculation Values and Test Results of the Electron Gun's Impedance

Key: 1. Calculation  
2. Test

Based on the above mentioned cathode emission mechanism, the cathode material should be selected of a material which has a high melting point and is hard. We used tantalum and the shape was an annular thin knife piece. The anode generally uses a material with a low atomic number so as to decrease as much as possible the loss caused by the electron beam being transformed into x-rays. In order for the electrons to easily pass through the anode tube wall, we used a seamless stainless steel tube with a wall thickness of  $30-50\mu\text{m}$ . After the electrons were calculated to have energy greater than 150keV, they could pass

through a stainless steel anode tube wall with a thickness of 50  $\mu$ m. When in 200 kV, we used the probe method to measure the electron beam flow. Its beam flow density was  $2.1\text{A}/\text{cm}^2$  (calculated by electron beam flow received by the probe surface). Its beam flow waveform is shown in fig. 4. This type of structure can sustain over 10 atm pressure.

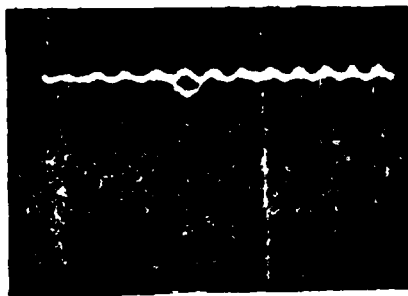


Fig. 4 The Electron Beam Waveform Measured When There is a Vacuum in the Anode and the Output of the Marx Generator is 200kV. Time Scale is 10ns.

#### Characteristics of the Electron Beam

We used the probe method to observe and study the beam flow characteristics of the radial electron beam passing through the cylindrical anode. The probe was an aluminum rod 0.3cm in diameter and 0.55cm in length.

When there was atm pressure air inside the anode, the typical waveform of the beam flow was as shown in fig. 5(a).

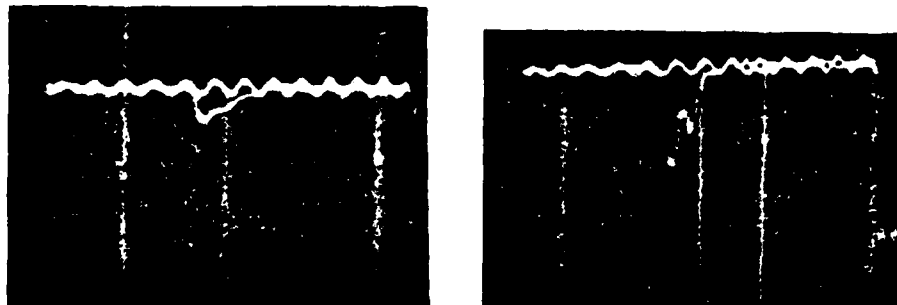


图5 典型的阳极内束流波形  
 (a) 阳极内为1个大气压空气时  
 (b) 阳极内真空时(时间为10ns)

Fig. 5 Typical Waveform of the Beam Flow Inside the Anode

Key: (a) When there is 1 atm pressure air  
 inside the anode  
 (b) When there is a vacuum inside the  
 anode (time is 10ns)

When the voltage is 510kV, the peak value of the beam flow is  $21A/cm^2$ . Fig. 6 is a comparison of the waveforms of the beam flow and voltage.

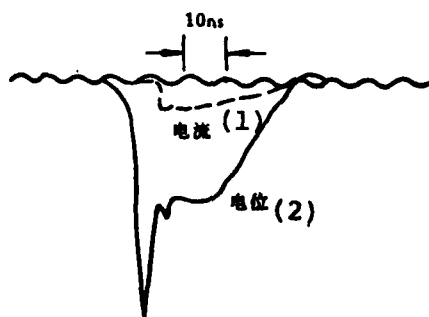


Fig. 6 Comparison of the Waveforms of the Beam Flow and Voltage

Key: 1. Electric current  
 2. Electric potential

The hysteresis of the beam flow is about 10ns as compared to the voltage. The relationship of the peak value of the beam

flow and the discharge voltage of the Marx generator is shown in curve 2 of fig. 7.

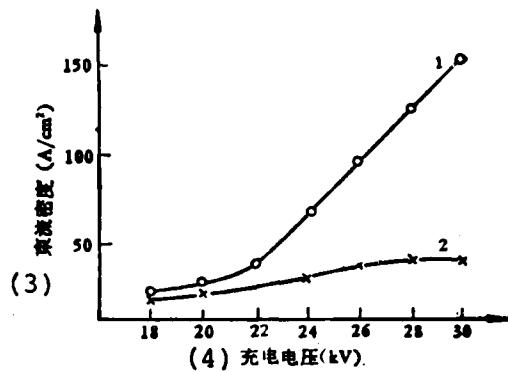


Fig. 7 Relationship of the Peak Value of the Beam Flow and the Discharge Voltage of the Marx Generator

Key:

- 1. Line 1 - Vacuum state
- 2. Line 2 - 1 atm pressure air
- 3. Beam flow density
- 4. Discharge voltage

We also observed the beam flow characteristics when there was a vacuum in the anode ( $\sim 10^{-4}$ ). The typical waveform is as shown in fig. 5(b). This waveform is obviously different from the waveform in the air (fig. 5(a)). The relationship of the peak beam flow and the discharge voltage of the Marx generator at this time is very different from the air as shown in curve 1 of fig. 7. We estimate that the electric current density of the anode surface is about  $150\text{A}/\text{cm}^2$  at this time.

We used acid-sensitive allochromatic sheets to qualitatively observe the space distribution of the electron beam along the axial direction. When observing, an allochromatic sheet with a width of 0.3cm was placed in the anode. When there was 1 atm pressure air in the anode, we obtained the blackness mark curve as shown in fig. 8. The non-uniformity along the axial direction was  $\sim \pm 10\%$ . When there is a vacuum in the anode, under

similar conditions, the acid-sensitive allochromatic sheet will become much deeper in color. In the same way, this shows that when there is air in the anode the beam flow is much smaller than when there is a vacuum.

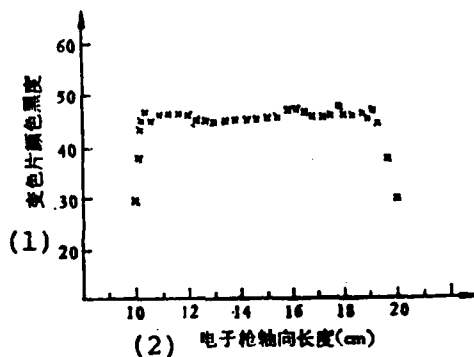


Fig. 8 Space Distribution of the Electron Beam on the Axial Direction

Key: 1. Blackness of allochromatic sheet  
2. Axial length of electron gun (cm)

Aside from this, when there is a vacuum in the anode, during each excitation, the change in front of the beam flow waveform is not large and relatively uniform. This shows that when an annular thin knife piece is used as the cathode, repeatability is better.

The above mentioned test results show that the radial electron beam possesses the following characteristics. Firstly, the beam flow obtained on the probe was smaller than the electron gun's beam flow. Secondly, when the anode is filled with air, the beam flow is smaller than when there is a vacuum state. These characteristics are similar to the results of Ramirez [7]. Further, there is a rather large disparity in the relationship between the beam flow when there is air filled in and a vacuum state in the anode and the discharge voltage of the Marx generator (i.e., the energy transmitted into the

electron gun). These facts show that after the radial electron beam passes through the cylindrical anode film, the characteristics of the radial convergence weaken and manifest similar tendencies in each direction [8]. Therefore, we cannot use the horizontal beam's one-dimensional directional physical model to explain the characteristics of the radial beam and measure its parameters. Although reference [8] has done preliminary discussions in this area, yet we still await further establishment and perfection of a physical model and test method.

We used the probe method to measure the radial electron beam with a beam flow of  $10-16\text{A}/\text{cm}^2$  (in 1 atm pressure air). We used it to pump argon-nitrogen compound gas to obtain the second positive band ultraviolet laser output of  $\text{N}_2$ ; the wavelength was  $3577\text{\AA}$  and  $3805\text{\AA}$  [9]. When the beam flow was lower than  $10\text{A}/\text{cm}^2$ , there was no laser output.

#### Conclusion

Use of radial electron beams to pump the  $\text{Ar-N}_2$  laser shows that whether obtained in reference [9] or reference [10], the total efficiency of the laser is always higher than the use of the horizontal beam as the pumping means as seen in reference [11].

The characteristics and testing of the radial electron beam still await further research. Physical models and test methods await establishment and perfection. The method which we presently use to measure the radial electron beam can be used to distinguish whether or not this type of beam has attained the requirements for pumping lasers.

After further improving the characteristics of the Marx generator so that it can operate with repeating pulses, we can obtain high average laser output power. At the same time,

we can realize multi-wavelength operating states [12].

The experiments and discussions carried out on the Marx generator using high pressure millimicrosecond electric pulse have certain reference value for expanding research on the use of the Marx generator in lasers and in other areas.

Finally, we would like to express our gratitude to those comrades who provided us with test conditions as well as who held scientific discussions with us.

#### References

- [1] J.B. Gerardo, et al., Proceedings of the International Topical Conf. on Electron Beam Research and Technology, Nov. 3-5 1975, Albuquerque, New Mexico, 2(1977), 169.
- [2] United States Patents 3,970,957.
- [3] Zhang Qi et al., Electronics News, 1(1979), 56.
- [4] G. A. Mesyai et al., authors, Fang Bo, tr., The Formation of High Pressure Millimicrosecond Pulses, Atomic Energy Publications, 1975.
- [5] I. Langmuir and K.B. Blodgett, Phys. Rev., 22(1923), 247.
- [6] L.G. Schlitt and L.P. Bralley, Proceedings of the International Topical Conf. on Electron Beam Research and Technology Nov. 3-5 1975, Albuquerque, New Mexico, 2 (1977), 239.
- [7] J.J. Ramirez et al., 2nd International Topical Conf. on High Power Electron and Ion Beam Research and Technology, Ithaca, New York 2(1978), 891.
- [8] J.J. Ramirez and K.R. Prestwich, J. Appl. Phys., 50(1979), 4988.
- [9] Xu Shanshan and Ge Qi, Electronics News, 3(1980), 144.
- [10] E.R. Ault, Appl. Phys. Lett. 26(1975), 619.
- [11] E.R. Ault, et al., IEEE J. QE-10(1974), 624.
- [12] E. R. Ault, Appl. Phys. Lett., 28(1976), 23.  
D. J. Bradley, et al., Opt. Commun., 14(1975), 1.

A. M. Vonnov, et al., Quantum Electronics, 4 (1977), 426.  
C. B. Edwards, et al., Rev. Sci. Instrum., 50(1979), 1201.